

Article

Not peer-reviewed version

---

# Matching Networks Design for Ultrasonic Guided Wave Interdigital Transducers

---

[Lorenzo Capineri](#) \*

Posted Date: 21 August 2025

doi: 10.20944/preprints202508.1492.v1

Keywords: interdigital transducer; matching network; ultrasonic guided wave; equivalent electric impedance; integrated driving electronic; network integration; structural health monitoring



Preprints.org is a free multidisciplinary platform providing preprint service that is dedicated to making early versions of research outputs permanently available and citable. Preprints posted at Preprints.org appear in Web of Science, Crossref, Google Scholar, Scilit, Europe PMC.

Copyright: This open access article is published under a Creative Commons CC BY 4.0 license, which permit the free download, distribution, and reuse, provided that the author and preprint are cited in any reuse.

Disclaimer/Publisher's Note: The statements, opinions, and data contained in all publications are solely those of the individual author(s) and contributor(s) and not of MDPI and/or the editor(s). MDPI and/or the editor(s) disclaim responsibility for any injury to people or property resulting from any ideas, methods, instructions, or products referred to in the content.

Article

# Matching Networks Design for Ultrasonic Guided Wave Interdigital Transducers

Lorenzo Capineri

Dipartimento Ingegneria dell'Informazione Università degli Studi di Firenze, Firenze, Italy1;

lorenzo.capineri@unifi.it

## Highlights

Analysis and design rules of a resonant matching network for ultrasonic guided wave interdigital transducers. Integrated implementation with a piezopolymer interdigital transducer and validation with low voltage power supply driving electronics.

### What are the main findings?

- Passive components matching network for interdigital guided wave transducers
- Transfer function analysis and design rules/method

### What is the implication of the main finding?

- Easier integration of interdigital transducers into structural health monitoring systems
- Driving electronic circuit with low power supply voltage

## Abstract

Ultrasonic guided waves interdigital transducers realized with piezoelectric materials are of interests for Structural Health Monitoring systems because their capability of Lamb wave mode selection respect to single element transducers. Besides this advantage the coverage of large areas with minimum number of elements is an important challenge and the problem of efficient excitation with integrated electronics must be solved. This work proposes an electrical matching network topology made of L and C passive components that can be designed for the tradeoff between electrical to mechanical conversion efficiency and bandwidth. The network circuit is analyzed considering the equivalents transducer impedance and the output impedance of the driving electronics. The design rules derived by the transfer function analysis are described and a case study for a piezopolymer IDT is presented. Finally with the implementation of the integrated matching network with the connector of the IDT the effect of cable capacitance is minimized. In conclusion the article is a contribution for using IDT efficiently and in a versatile mode for different electronic front-ends that usually operate at low power supply voltage.

**Keywords:** interdigital transducer; matching network; ultrasonic guided wave; equivalent electric impedance; integrated driving electronic; network integration; structural health monitoring

## 1. Introduction

Ultrasonic guided wave interdigitated transducers (UGWIDT) are increasingly used in SHM systems [1–3] for the monitoring of both composite [4,5] and metallic [6] laminar structures, due to their ability to select propagation modes useful for detecting and monitoring mm- and sub-mm-sized defects.

To cover large areas with a limited number of transducers, it is necessary to be able to shape the beam while simultaneously ensuring high transmitted power to ensure a good signal-to-noise ratio [7,8]. To maximise the power the UGWIDT must be well matched with the driving electronics.

UGWIDTs are piezoelectric devices designed to operate at defined frequencies with narrow bandwidth (typically tens of kHz). Typically, SHM systems are designed with operating frequencies

selected in the 100 kHz–1 MHz range based on the characteristics of the laminate and therefore the dispersion curves.

Fabricating UGWIDTs with thin (20  $\mu\text{m}$ –200  $\mu\text{m}$ ) piezoelectric materials (piezopolymer films [5], spray deposition [9], piezocomposite [10]) in the above frequency range, results in a non-resonant piezoelectric device, meaning its equivalent electrical impedance is well approximated by an ohmic-capacitive impedance

$Z_L = R_L + 1/j\omega C_L$ . The resistive part of the impedance  $R_L$  represents the conversion of electrical excitation power into mechanical power and includes also the piezoelectric material losses; the capacitance  $C_L$  depends on the dielectric constant of the piezoelectric material, the thickness, and the area of the electrode design and it is frequency dependent.

The objective of this work is to analyze a modified version of a resonant matching network inserted between the driving circuit and the impedance of UGWIDT. The design goal is to achieve a compromise between the desired bandwidth and power transfer/conversion, also considering the characteristics of the driving electronic circuit while keeping the network as simple as possible. From the following analysis, a design methodology is proposed that allows UGWIDTs to be driven with low-voltage driver circuits (e.g., <24 V), with the advantage of avoiding high-voltage power supply circuits.

Matching networks for UGWIDTs require alternative solutions to those traditionally used for ceramic resonant transducers [11,12]. For the latter, a compensating inductor is used, either in parallel or in series with the transducer. Its electrical impedance is well represented by the resonant circuit model proposed by Kino-Mason in [11]. As is well known, for these transducers, the value of the compensating inductance essentially cancels the effect of the capacitive component at the resonant frequency (series or parallel) and make the load impedance equivalent purely resistive. For narrowband systems, matching networks are used to adapt the transducer impedance to the front-end electronics and typically for single-element transducers passive networks with L, C and magnetic transformers components are used. The magnetic transformer solution is well known but requires the replication of transformers for the number of elements that constitute the UGWIDTs network of the SHM system. In addition to the poor repeatability of the characteristics and the cost, there is an increase in weight and the reliability factor that discourages the adoption of this solution. However, the advantage of the transformer lies in the possibility of increasing the excitation voltage of the piezoelectric transducer starting from a driving with low voltage signals. The matching network design for wide bandwidth piezoelectric transducers is even more complex network [13] and a recent review of the matching network for ultrasonic transducers is reported in [14].

In the case of UGWIDT transducers, the classic solutions mentioned above can be adopted, but since the resistive portion of the impedance is generally higher than that of ceramic transducers, it is difficult to transfer electrical power to a high-value resistive load without increasing the excitation voltage to such values that require a more complex electronic driving circuit. Furthermore, the ideal matching network should be able to match different values of the output impedance of the driving circuit, which can vary greatly depending on the solution adopted: pulsers with power MOSFET devices or linear amplifiers [15,16]. This aspect will also be considered when choosing the matching network topology.

This paper presents a solution that introduces a resonant matching network with the UGWIDT equivalent impedance in parallel to the inductor of the resonant circuit. A matching network design methodology is presented that can be applied to different UGWIDT fabrication technologies based on bandwidth, source impedance, and conversion efficiency requirements.

Finally, the presented design solution, based only on passive L and C components, will also be evaluated for an integrated implementation on the UGWIDT connector to minimize costs, size, and weight. Some examples are therefore reported in the experimental section regarding UGWIDTs made of piezopolymer film (PVDF), since this material is very versatile for the construction of SHM systems but is not as efficient at generating UGWs compared to piezocomposite materials.

## 2. Matching Network with a Double Tuning Resonant Circuit

For an UGWITD it can be assumed that according to the interdigital finger geometry shown in Figure 1, the equivalent electrical capacitance can be estimated by the well-known formula:

$$C_L = \epsilon_0 \epsilon_r \frac{A}{t} \quad (1)$$

where  $t$  is thickness of the piezoelectric material,  $A$  active area of the UGWITD and  $\epsilon_r$  is the relative dielectric constant of the piezoelectric evaluated at the operating frequency  $f$  and temperature  $T$ .

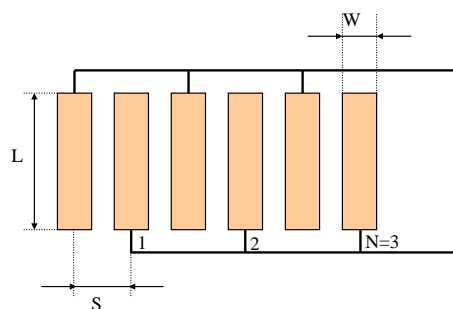


**Figure 1.** Dimensional parameters of the finger electrodes for a UGWITD. In the example the number of finger pairs  $N$  is 3.

According to Figure 1, active area  $A$  can be calculated as:

$$A = L * W * N \quad (2)$$

By applying the KLM model [11] for an IDT, the equivalent resistance  $R_L$  of the electrical impedance can be estimated to be associated to the conversion of the active electrical power provided to the UGWITD and the power losses of the material at the given operating temperature  $T$  and frequency  $f$ .

The matching network circuit proposed in this work is based on a composite resonant L-Ca circuit where the transducer impedance  $Z_L$  is connected in parallel to the inductor  $L$ , as shown in Figure 2. The advantages of this topology will be explained in the following, but we can immediately notice that the capacitor  $C_a$  provides isolation from the eventual DC component in the driving signal  $V_{in}$  and the inductor  $L$  is a short circuit for the DC components of  $V_{out}$ . For completeness of the topic the solution for a matching network of a capacitive – resistive load to a resistive voltage source can also be done with two inductors [17], ( $C_a$  is replaced by a second inductor) but it is more expensive, bulky and it is a short circuit for the eventual DC component in the driving signal  $V_{in}$ .

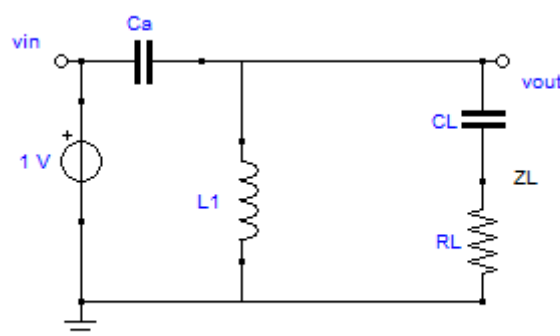


**Figure 2.** The equivalent transducer impedance  $Z_L$  connected in parallel to the inductor  $L$ .

The transfer function of the circuit shown in Figure 2 can be solved by MATLAB symbolic equation tools and can be obtained the following expression in the Laplace domain ( $s=j\omega=j2\pi f$ ):

$$H_1(s) = \frac{V_{out}}{V_{in}} = \frac{sL R_L + L/C_L}{sL R_L + \frac{R_L}{sC_a} + L \left( \frac{C_L + C_a}{C_L C_a} \right) \left[ 1 + \frac{1}{s^2 L (C_L + C_a)} \right]} \quad (3)$$

The analysis of the denominator of (3) shows a main resonant effect for the angular frequency  $\omega_1 = \frac{1}{\sqrt{L(C_L + C_a)}}$ .

The transfer function evaluated for  $\omega_1$  is simplified to two terms and can be analyzed for new insights relative to the design of the matching network.

$$H_1(s_1 = j\omega_1) = \frac{V_{out}}{V_{in}} = \frac{s_1 R_L + 1/C_L}{s_1 R_L \left[ 1 + \frac{1}{s_1^2 L C_a} \right]} = - \left( 1 + \frac{1}{s_1 C_L R_L} \right) \frac{C_a}{C_L} \quad (4)$$

In (4) we can observe that the first term in brackets depends only on the UGWIDT electrical impedance determined by  $C_L$  and  $R_L$ , and the second term represents a gain factor  $G = \frac{C_a}{C_L}$  that can be adjusted by the choice of  $C_a$ . Once  $C_a$  is defined, the desired value for  $\omega_1$  can be tuned by the value of  $L$ . The possibility to tune  $C_a$  and  $L$  separately is the advantage of the proposed circuit topology for the matching network.

The increase in the gain factor by  $C_a$  causes a decrease of the input impedance  $Z_{in}$  at the input port  $V_{in}$  (see Figure 2) as reported in (5):

$$Z_{in}(s) = \frac{V_{out}}{I_{in}} = \frac{sL R_L + L/C_L}{sL + \frac{1}{sC_L} + R_L} + \frac{1}{sC_a} \quad (5)$$

In (5) we also observe that the variation of  $C_a$  and  $L$  have independent effects on the two additive terms. Moreover, a decrease of  $Z_{in}$  has the effect of partitioning the open circuit available voltage  $V_s$  of the driving circuit with the finite value of output impedance  $Z_s$  as shown in Figure 3.

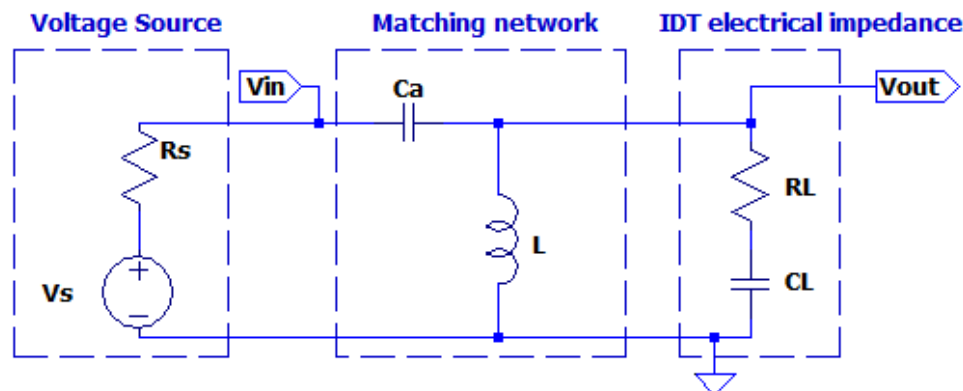


**Figure 3.** Matching network connected with the input port Loading effect of input port  $V_{in}$  to the source  $V_s$ ,  $R_s$  and the electrical impedance of the UGWIDT at the output port  $V_{out}$ .

In (5) the denominator shows a series resonant effect on the impedance with a local maximum at the angular frequency  $\omega_2 = \frac{1}{\sqrt{LC_L}}$ . The difference between  $\omega_1$  and  $\omega_2$  depends on the  $G$ ; this double resonant effect must be considered for the design of the matching network and exploited to obtain the best trade-off.

Ideally a matching network is connected directly to the source (driving electronic circuit) with with different output impedance  $R_s$ . In practice the matching network will be connected to the source and the UGWIDT by cables with the line impedance. For the frequency range of interest, we can



simplify the effect of the connection line with a capacitor  $C_b$  in parallel at the input port  $V_{in}$  of the matching network (see Figure 4). We anticipate this circuit that will be treated in detail in section 2.

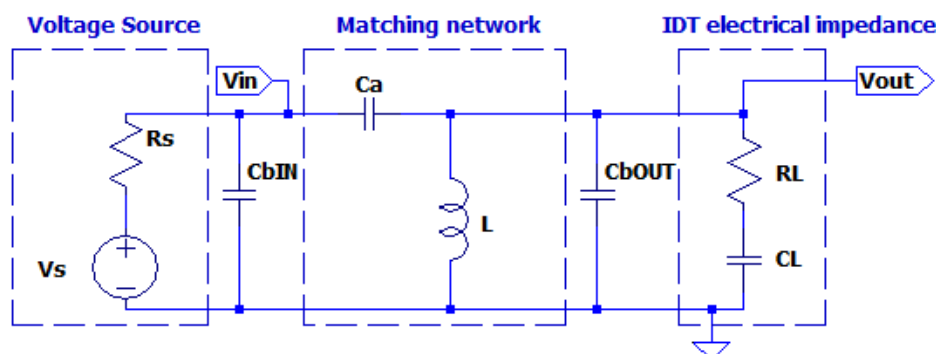


**Figure 4.** Schematic circuit for considering the capacitive effect of  $C_b$  due to connection cable of the matching network at the input or at the output.

For the sake of completeness, we can observe that the series of capacitors  $C_a$  and  $C_b$  forms a voltage divider for  $V_{out}$ ; this circuit network is for matching load at radiofrequency solving the problem of tuning and matching separately [18]. The higher values of  $C_a$  (up to several nF) has an impact on the circuit footprint, volume and cost but the value of the desired resonant frequency is obtained with a lower value of  $L$ , which is an advantage especially when current in order of 0.1A – 1 A are required for driving with sufficient power the UGWIDT.

## 2.1. Parametric Simulations of the Matching Network

### 2.1.1. UGWIDT Electrical Impedance

In this work we consider the design of an UGWIDT with finger electrode pitch  $S=4\text{mm}$  operating at 450 kHz for defect detection in a Carbon Fiber Reinforced Plastic (CFRP) laminate. The electrode design characteristics are reported in Figure 1. The dimensions of the finger electrodes are  $S=4\text{mm}$ ;  $W=1,5\text{ mm}$ ;  $L=14\text{mm}$ ;  $N=3$ . The corresponding central wavelength  $\lambda = 2 S = 8\text{ mm}$ . The piezopolymer film was a gold metallized PVDF film with thickness  $t=100\text{ }\mu\text{m}$  and the finger electrodes geometry shown in Figure 1 realized by laser ablation [19]. The UGWIDT electrical impedance was measured with the UGWIDT mounted on the CFRP cross-ply laminate as shown in Figure 5.



**Figure 5.** Measurement of the equivalent electrical impedance at 450 kHz with volt-amperometric method (Voltage probe TEKTRONIX Mod. P3010, current probe P6022 TEKTRONIX). The piezopolymer UGWIDT is bonded to the CFRP cross ply laminate.

The results for the electrical impedance is a series circuit  $C_L = 210 \text{ pF}$ ,  $R_L = 2000 \Omega$ . This pair of values for  $C_L$  and  $R_L$ , corresponds to the electrical impedance of one section of the UGWIDT measured either from V+ or V- to ground (GND), as shown in Figure 6

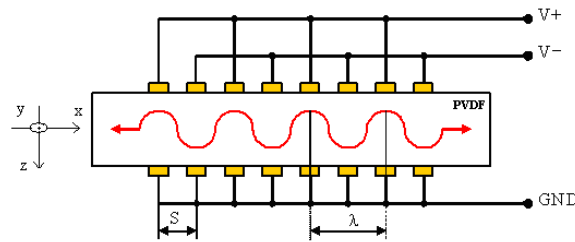


**Figure 6.** Differential driving V+ and V- of the UGWIDT.

In the next section we will use these values for parametric simulations to explain the results of the formal analysis of the transfer functions.

### 2.1.2. Parametric Simulations for $C_a$ , $R_s$

The first parametric simulation regards the matching network shown in Figure 3.

The aim is the evaluation of the influence of the choice of the value of  $C_a$  for the fixed values of  $C_L$  and  $R_L$ .

The value of  $L=120 \mu\text{H}$  is determined by the desired value  $\omega_1 = 2\pi f_1$ , where  $f_1 = 450 \text{ kHz}$  as reported in section 2.1. We consider also an inductor series resistance  $\text{ESR}=0.16 \Omega$  derived from data sheet of a commercial component. The source resistance  $R_s=4 \Omega$  is initially chosen considering a linear power amplifier [20,21]. By the definition of  $\omega_1$  that depends on  $C_L$ ,  $L$ ,  $C_a$  is expected a variation of  $\omega_1$  with the parametric simulation for  $C_a$ . The analysis of transfer function  $H_1(s)$  around 450 kHz will point out this behavior of the  $H_1(s)$  magnitude according to (4).

In Figure 7 is reported the simulated magnitude of the transfer function  $H_1(s)$  for  $C_a = 600 \text{ pF}, 700 \text{ pF}, 800 \text{ pF}, 900 \text{ pF}, 1000 \text{ pF}$  from right to left.

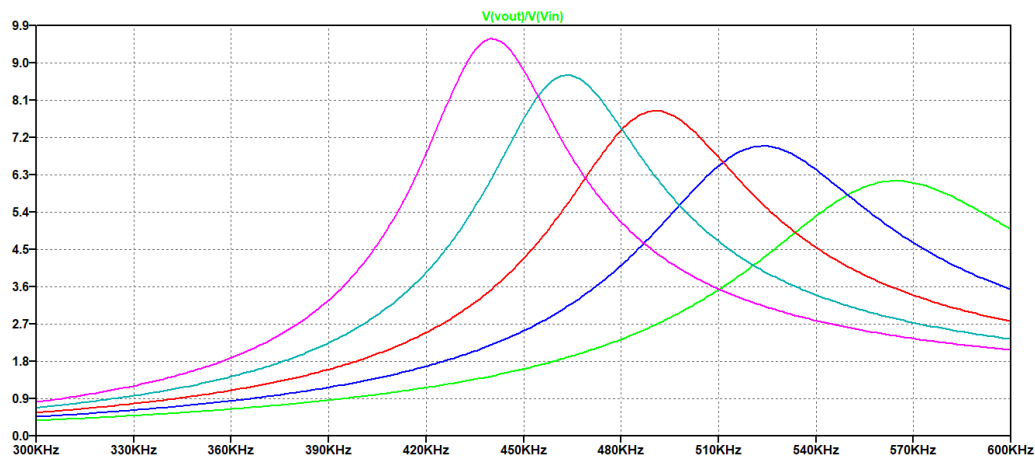


**Figure 7.** Simulated transfer function  $H_1(s)$  with parametric simulations for  $C_a$ .

From Figure 7 we observe that the maximum value of the transfer function increases with  $C_a$  and the evaluation of the magnitude at 450 kHz is reported in the following Table 1.

**Table 1.** |  $H_1(s)$  | @ f=450 kHz.

$C_a$	$H_1(s)$	G
600 pF	1,62	2,85
700 pF	2.57	3,33
800 pF	4.27	3,80
900pF	7.6	4,20
1000pF	8.79	4,76

Choosing the higher value of  $C_a$  equal to 1000 pF provides an amplitude gain factor  $G= 4.76$  and a transfer function amplitude of 8.79. This value of  $C_a$  is not a limit for the choice, but it is a good compromise for the component footprint and parasitic.

Figure 6 shows also the effect on the bandwidth of the driving signal that must match the UGWIDT requirements. Higher values of  $C_a$  provide narrower bandwidth: for  $C_a =1000\text{pF}$  the -3dB bandwidth is 45kHz while for  $C_a =600\text{pF}$  is 72 kHz.

Another important factor for the analysis of the matching network is the effect of variation of the source impedance  $R_s$ . Different driver circuits can have low value as  $0.4\ \Omega$ , representing for example the case of a MOSFET integrated pulser, much lower to the initially assumed value of  $4\ \Omega$  for a linear power amplifier. Then a parametric simulation has been done for three values of  $R_s = [0.4,1, 4]\ \Omega$  with a fixed value of  $C_a =1000\text{pF}$ . The voltage source  $V_s$  (see Figure 3) has 15V amplitude, being compatible with integrated driving circuits. The evaluation of the voltage amplitude  $V_{out}$  at the load is reported in Table 2.

**Table 2.**  $V_{out}$  @450 kHz.

$R_s\ [\Omega]$	$V_{out}\ [\text{Volt}]$
0.4	133.2
1	129.6
4	121.5

The results in Table 2 validate the approach of having a matching network that increases the input voltage from 15 V of a factor 8.7 and is largely independent from the source resistance  $R_s$ .

2.1.3. Capacitive Effect of Connection Cable and refinement of  $C_a$

In the theoretical analysis we neglected the effect of the connection cable between the driving electronic circuit and the UGWIDT. In general, this connection for a differential driving of and UGWIDT (see  $V_+$  and  $V_-$  in Figure 6) is realized with a twisted pair shielded cable. Depending on the length and dielectric of the insulation materials, we evaluated the capacitance in parallel to the transducer of about  $C_{bOUT}=170\ \text{pF}$  for 1.2 m length.

Including the cable capacitance in the simulation (see Figure 8), the value of  $C_a$  must be optimized for the operating frequency of 450 kHz. In the solution proposed in Figure 8, the matching network is located on the board of the electronic circuit and the signal  $V_{out}$  and GND are connected to the transducer by the connection cable. As we will see later in this article, the integration of the matching network on the UGWIDT connector is more convenient because the effect of cable capacitance is reduced.



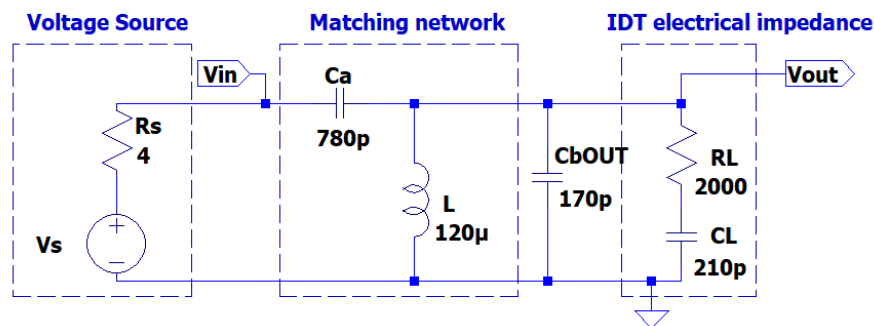


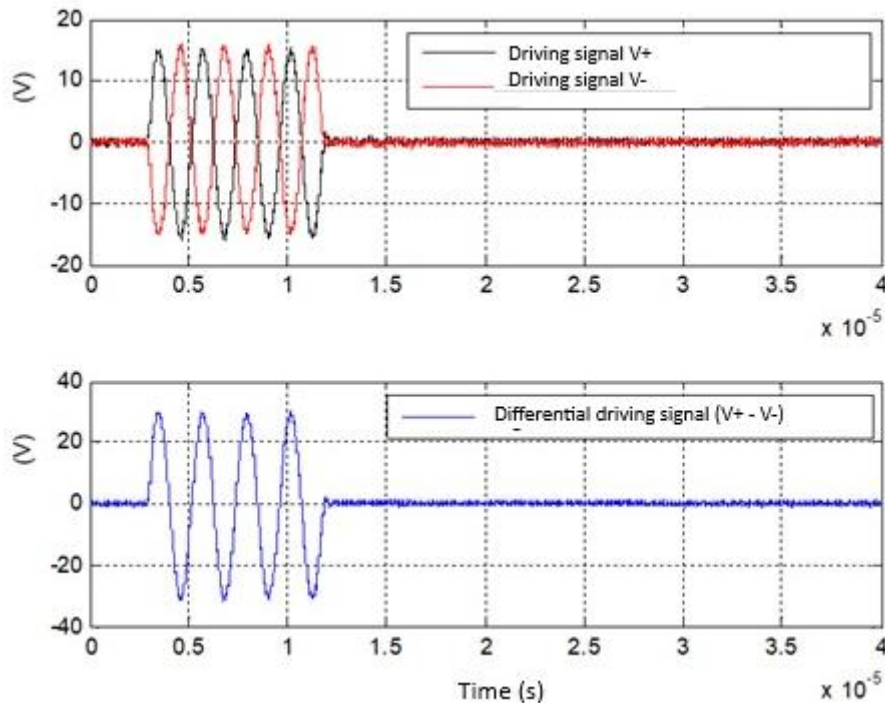
**Figure 8.** Simulated matching network including connection cable capacitance  $C_{bOUT}=170\text{pF}$ .

For the optimization we select by parametric simulation an optimal value of  $C_a = 780\text{pF}$  which maintains a high output voltage  $V_{out}$  on the transducer of 105 V. Accounting for this effect the transfer function magnitude is  $105/15=7$ , lower than 8.79 as evaluated in Table 1 without considering the cable capacitance.

## 2.2. Experimental Validation of the Matching Network

The designed matching network has been mounted onto the PCB of the driving circuit that is a power linear amplifier [22] and connected with a shielded cable to the UGWIDT described in previous section.

The driving differential signals ( $V_+$  and  $V_-$ ) applied to each section of the UGWIDT (see Figure 6) are shown in Figure 9 (top).



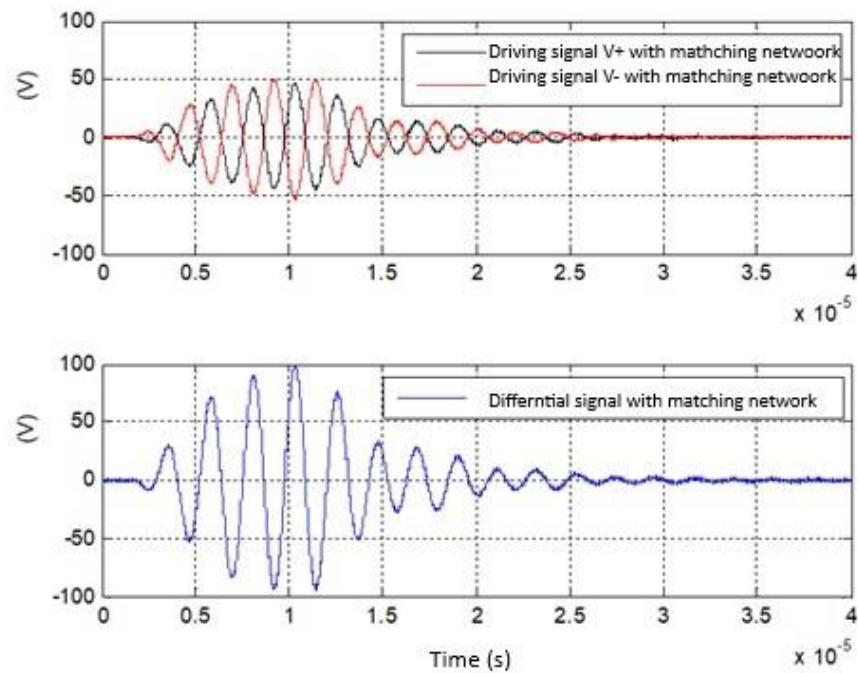


**Figure 9.** (Top) driving signals from a linear power amplifier. (Bottom) driving signals with the matching network shown in Figure 8.

The experimental results in Figure 9 (top) show driving signals with amplitude 15.5V amplitude and in Figure 9 (bottom) the corresponding signals after the insertion of the matching network with amplitude of about 100V. The transfer function magnitude experimentally evaluated is  $100/15.5=6.45$ . The estimate is in good agreement with simulations considering that some parasitic of passive components are not considered in the simulations.

### 2.3. Evaluation of the Input Impedance $Z_{in}$ .

The last part of the analysis concerns the estimation of the input impedance at the input port of the matching network.

In Figure 10 the magnitude of the impedance has been simulated, and the minimum is obtained at 450 kHz and its value about 59Ω.

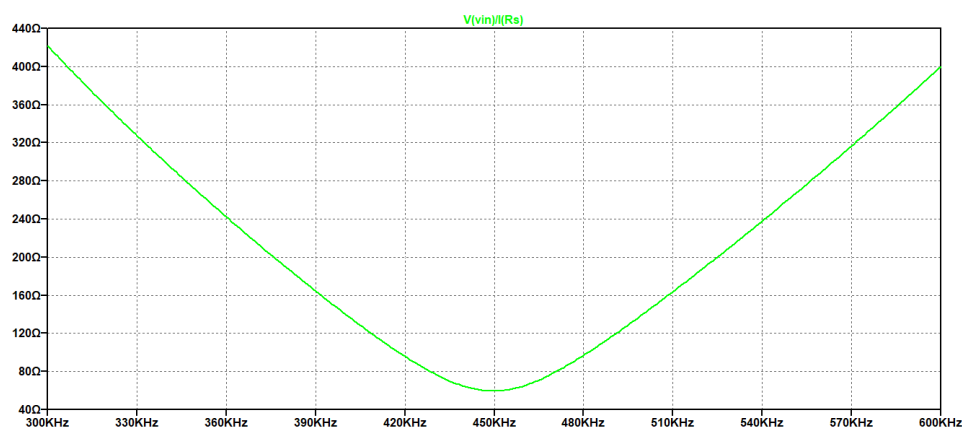


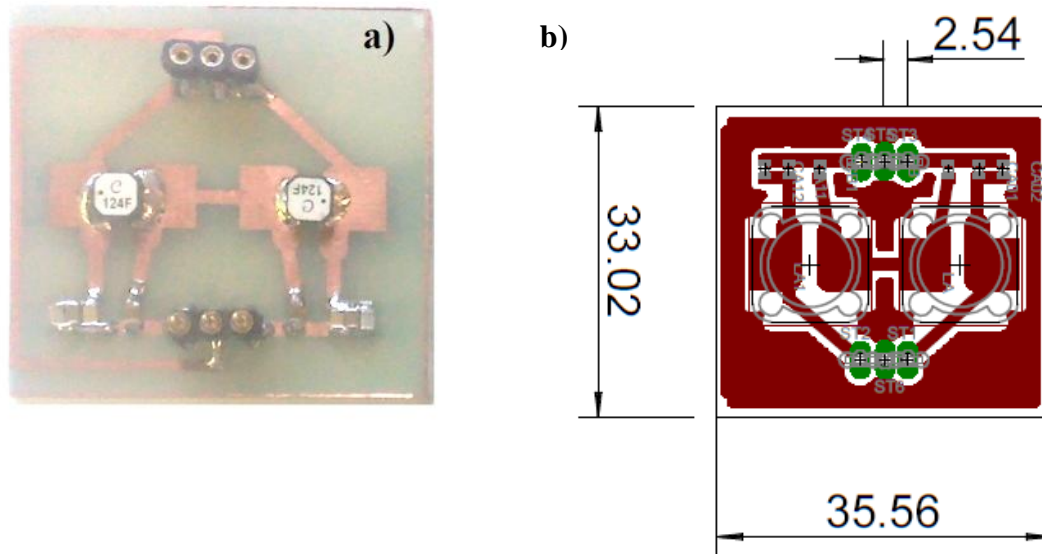
**Figure 10.** Magnitude of the input impedance  $Z_{in}$  with the matching network.

The minimum of  $Z_{in}=60\Omega$  confirm the little influence of the source impedance that is in general much lower than this value. Then this design approach is versatile for different driving electronic circuits.

### 3. Integration of the Matching Network on the UGWIDT Connector

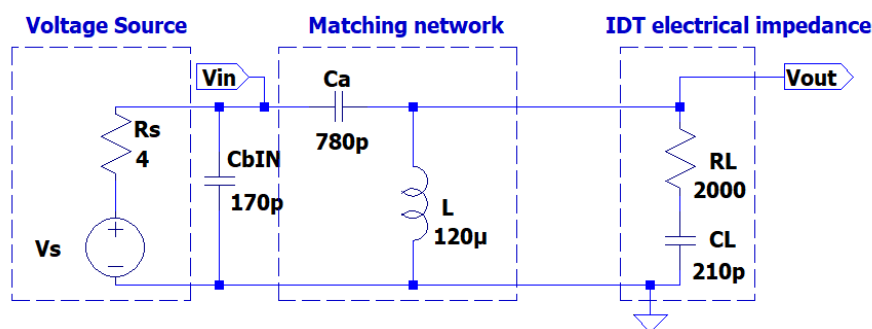
In section 2.1.2 the effect of the cable used for the connection between the matching network and the UGWIDT is pointed out. An alternative approach is the realization of the matching network on a PCB that is also used to connect metal fingers to the driving signals. The type of contact between top and bottom PCBs with copper pads and the gold metallized PVDF is guaranteed by the pressure generated by microrivets joining the two PCBs and the PVDF film in the middle [3]. On one of the two PCBs the circuit of the matching network is mounted with low profile, low weight SMD components.

In Figure 11 is illustrated the PCB design and the mounted matching network.



**Figure 11.** (a) Final assembly of the matching network with differential output and ground . (b) PCB design for the connector with integrated matching network; dimensions are in mm.

With this change in the connection, now the cable capacitance must be moved in parallel to the input of the matching network as shown in Figure 12.



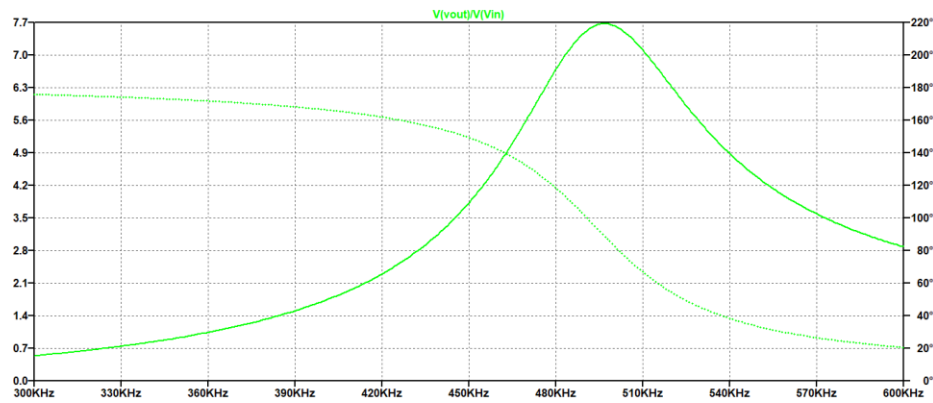


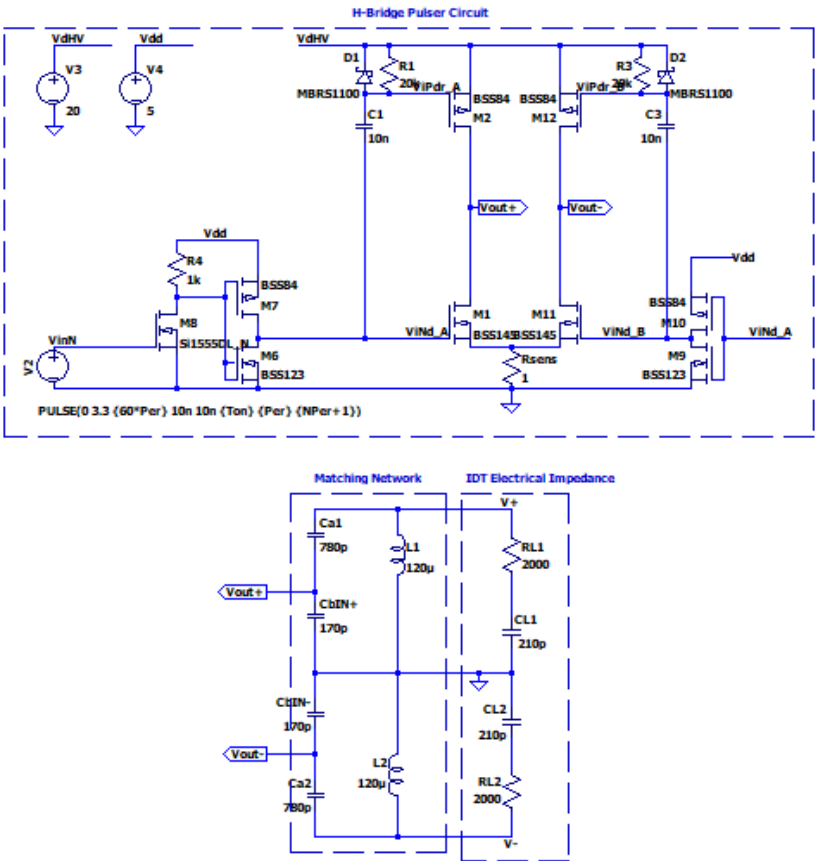
**Figure 12.** (Top) schematic of the matching network including connection cable capacitance  $C_{bin}=170\text{pF}$  to the driving electronics. (Bottom) Simulated transfer function magnitude.

In the bottom of Figure 12 we can see that at 450 kHz the gain factor evaluated on the magnitude of  $H_1(s)$  is 3.8. By simulation we can also observe a change of the  $Z_{in}$  that is increased to  $91\Omega$  at 450 kHz while the minimum equal to  $51\Omega$  is shifted to 494 kHz. The higher value of the input impedance means the requirement of higher input driving voltage to increase the current in  $R_L$ . This problem will be tackled in the next section.

#### 4. Pulser Circuit with Matching Network

In the previous section we concluded that the matching network can be designed with adequate gain factor and bandwidth, but the high input impedance limits the power delivered to  $R_L$ . For this inconvenience, a driving circuit based on an H-bridge with four power MOSFET is an effective solution. This type of electronic circuit is now common also in integrated devices and they can be supplied with a single power supply voltage [23–26]. The output voltage is doubled across the load thanks to the differential connection.

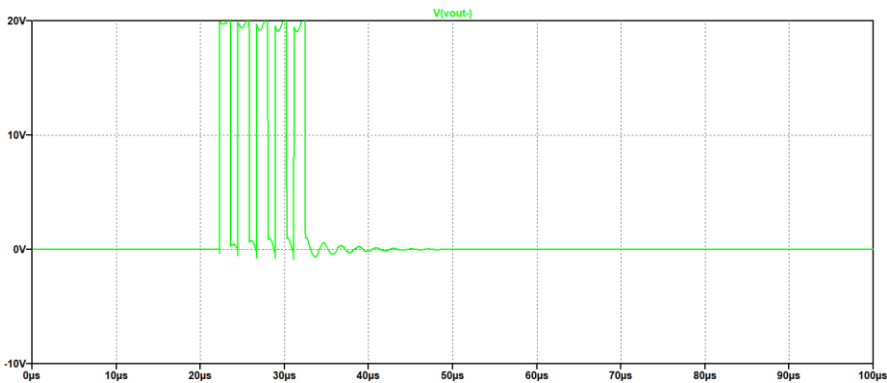
In a previous project we developed a modular system for exciting array of 16 IDTs [27]. Here we use the same board to test the effectiveness of the matching network for UGWIDT. In Figure 13 the schematic circuit for the simulation is shown.



**Figure 13.** Simulation of an H-bridge pulser circuit connected to the matching network with a cable capacitance of 170pF.

The excitation signal is a burst of 4 pulses at 450 kHz at 5V. These pulses are then processed to get out of phase correspondent signal by a CMOS inverter (see bottom right of Figure 13). The driving signals (Vleg+ and Vleg-) are obtained with a power supply voltage Vdd=20V. The output signals at the UGWIDT are Vout+ and Vout-.

In Figure 14 the results of the simulations are illustrated.



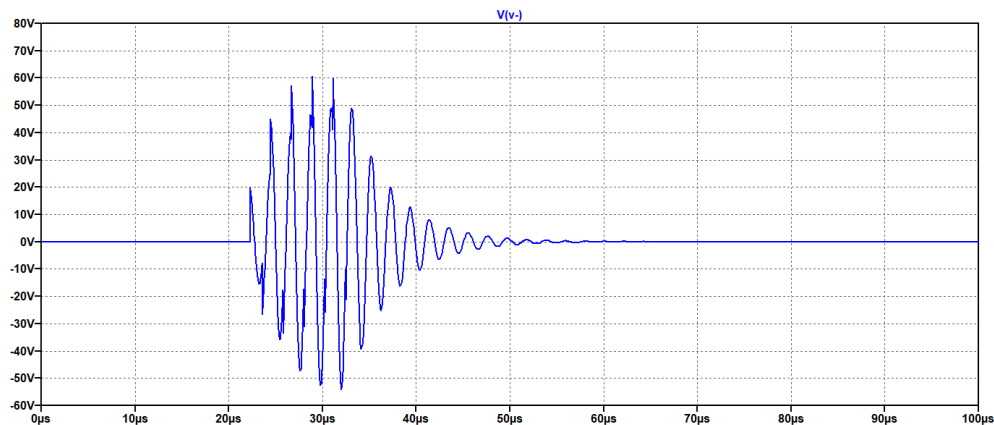


**Figure 14.** Simulation results of the excitation with an H. bridge supplied at 20V. (top) Driving signal for one section of the H-Bridge (bottom) Applied output voltage  $V_+$  to one section of the UGWIDT.

By simulation we can observe that a burst with an amplitude of 20 V generates a driving signal at one section of the UGWIDT of about 54V. The evaluation of the magnitude is  $54/20=2.7$ . The peak to peak is about 108V. The pulser circuit with differential driving recovers from the limitation of the integrated linear power amplifiers that can drive up to 24V the load at the maximum current.

The simulated results need also to be validated with an electronic circuit board implementing the H-bridge circuit shown in Figure 13 and the matching network realized on a PCB for connecting the piezopolymer UGWIDT.

In Figure 15 are presented the excitation signal with 4 pulses at 450 kHz with 20V amplitude and the corresponding signal on one section of the UGWIDT.

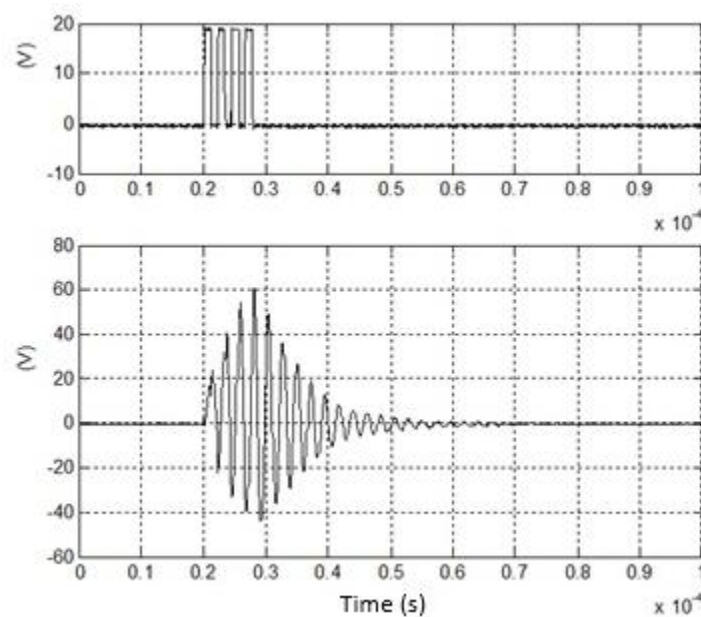


**Figure 15.** (top) Excitation burst applied to one input of the differential matching network shown in Fig.,13 (Bottom) Output signal applied to one section of the UGWIDT.

The comparison of the simulations and the experimental results shows that the gain factor and the shape of the output signal are in good agreement, and this solution can be adopted efficiently for driving the input impedance of the matching network.



## 5. Conclusions

The design of matching networks of UGWIDT fabricated with piezopolymer film is presented. Because of their relatively high impedance at the operating frequencies for SHM system and the low amplitude of the driving signals generated by integrated electronics, a matching network based on a resonant behavior is proposed and analyzed for the specific user case. The theoretical analysis of the transfer function and the input impedance provides insight on how to select the two main components L and Ca of this matching network with the load inserted in parallel to the inductor. In this way we can design separately the value of L for the desired operating frequency and the value of Ca for the voltage amplitude gain factor. The matching network is simple and provides a relatively high impedance with respect to the source, minimizing the effect of performance change depending on the driving electronics. Finally, the solution with an integrated matching network on the UGWIDT connector is presented and the full experimentation with a H bridge pulser demonstrates the effectiveness of this simple solution. The driving voltage up to 100 Vpp can be achieved increasing the signals generated from integrated power amplifiers or pulser, typically in the order of 24V. The design rules and the main trade off are reported so that the design of this type of matching network can be extended for UGWIDTs fabricated with other piezoelectric materials.

**Funding:** This research received no external funding.

**Conflicts of Interest:** The author declare no conflicts of interest.

## Abbreviations

The following abbreviations are used in this manuscript:

UGWIDT	Ultrasonic Guided Wave Interdigital Transducer
SHM	Structural Health Monitoring
IDT	Interdigital Transducer
PCB	Printed circuit board
PVDF	Polyvinylidene difluoride

## References

1. T. Stepinski, M. Mańka, and A. Martowicz, "Interdigital lamb wave transducers for applications in structural health monitoring," *NDT & E International*, vol. 86, pp. 199–210, Mar. 2017, doi: <https://doi.org/10.1016/j.ndteint.2016.10.007>
2. B. Ren and C. J. Lissenden, "PVDF Multielement Lamb Wave Sensor for Structural Health Monitoring," in *IEEE Transactions on Ultrasonics, Ferroelectrics, and Frequency Control*, vol. 63, no. 1, pp. 178–185, Jan. 2016, doi: [10.1109/TUFFC.2015.2496423](https://doi.org/10.1109/TUFFC.2015.2496423)
3. P. Giannelli, A. Bulletti and L. Capineri, "Multifunctional Piezopolymer Film Transducer for Structural Health Monitoring Applications," in *IEEE Sensors Journal*, vol. 17, no. 14, pp. 4583–4586, 15 July 2017, <https://doi.org/10.1109/JSEN.2017.2710425>.
4. M. Mańka, A. Martowicz, M. Rosiek, T. Stepinski, and T. Uhl, "Tunable interdigital transducers made of piezoelectric macro-fiber composite," *Smart Materials and Structures*, vol. 25, no. 11, p. 115022, Oct. 2016, doi: <https://doi.org/10.1088/0964-1726/25/11/115022>
5. A. Bulletti, P. Giannelli, M. Calzolari and L. Capineri, "An Integrated Acousto/Ultrasonic Structural Health Monitoring System for Composite Pressure Vessels," in *IEEE Transactions on Ultrasonics, Ferroelectrics, and Frequency Control*, vol. 63, no. 6, pp. 864–873, June 2016, doi: [10.1109/TUFFC.2016.2545716](https://doi.org/10.1109/TUFFC.2016.2545716).
6. B. Ren, H. Cho, and C. Lissenden, "A Guided Wave Sensor Enabling Simultaneous Wavenumber-Frequency Analysis for Both Lamb and Shear-Horizontal Waves," *Sensors*, vol. 17, no. 3, p. 488, Mar. 2017, doi: <https://doi.org/10.3390/s17030488>.
7. V. Giurgiutiu, *Structural Health Monitoring with Piezoelectric Wafer Active Sensors*. Academic Press, 2014.

8. X. Qing, W. Li, Y. Wang, and H. Sun, "Piezoelectric Transducer-Based Structural Health Monitoring for Aircraft Applications," *Sensors*, vol. 19, no. 3, p. 545, Jan. 2019, doi: <https://doi.org/10.3390/s19030545>
9. Shifeng Guo et al. 2019 Smart Mater. Struct. 28 075031, DOI 10.1088/1361-665X/ab1e88
10. Tadeusz Stepinski, Michał Mańka, Adam Martowicz, Interdigital lamb wave transducers for applications in structural health monitoring, *NDT & E International*, Volume 86, 2017, Pages 199-210,, ISSN 0963-8695, <https://doi.org/10.1016/j.ndteint.2016.10.007>
11. Kino, Gordon S. (1987). *Acoustic Waves: Devices, Imaging, and Analog Signal Processing*. Prentice-Hall. ISBN 0130030473.
12. A. R. Selfridge, R. Baer, B. T. Khuri-Yakub and G. S. Kino, "Computer-Optimized Design of Quarter-Wave Acoustic Matching and Electrical Matching Networks for Acoustic Transducers," 1981 *Ultrasonics Symposium*, Chicago, IL, USA, 1981, pp. 644-648, doi: 10.1109/ULTSYM.1981.197701.
13. L. Capineri, L. Masotti, M. Rinieri and S. Rocchi, "Ultrasonic transducers as a black-box: equivalent circuit synthesis and matching network design," in *IEEE Transactions on Ultrasonics, Ferroelectrics, and Frequency Control*, vol. 40, no. 6, pp. 694-703, Nov. 1993, doi: 10.1109/58.248213.
14. V. T. Rathod, "A Review of Electric Impedance Matching Techniques for Piezoelectric Sensors, Actuators and Transducers," *Electronics*, vol. 8, no. 2, p. 169, Feb. 2019, doi: <https://doi.org/10.3390/electronics8020169>.
15. H. Zhou, S. H. Huang, and W. Li, "Electrical Impedance Matching Between Piezoelectric Transducer and Power Amplifier," *IEEE Sensors Journal*, vol. 20, no. 23, pp. 14273–14281, Dec. 2020, doi: <https://doi.org/10.1109/jsen.2020.3008762>.
16. <https://www.analog.com/media/en/technical-documentation/data-sheets/lt1210.pdf> 15 August 2025
17. M. M. Weiner, *Monopole Antennas*, Marcel Dekker, Inc., CRC Press, Rev. Exp edition, New York, pp.110-118, 2003.
18. Valery Godyak , RF discharge diagnostics: Some problems and their resolution *J. Appl. Phys.* 129, 041101 (2021); doi: 10.1063/5.0024258
19. L. Bergamaschi, A. Bulletti, M. Dimitri and L. Capineri, "Modelling the beam pattern of piezopolymer interdigital transducers (IDT) for optimizing the off-axis response," 2022 *IEEE International Ultrasonics Symposium (IUS)*, Venice, Italy, 2022, pp. 1-2, doi: 10.1109/IUS54386.2022.9958806.
20. L. Svilainis and G. Motiejunas, "Power amplifier for ultrasonic transducer excitation," vol. 58, no. 1, pp. 30-36, Mar. 2006, doi: <https://doi.org/10.5755/j01.u.58.1.16970>.
21. L. Capineri, "A 15 MHz bandwidth, 60 Vpp, low distortion power amplifier for driving high power piezoelectric transducers," *Review of Scientific Instruments*, vol. 85, no. 10, p. 104701, Oct. 2014, doi: <https://doi.org/10.1063/1.4897155>.
22. J. Zhou and Y. Zheng, "Broadband Linear High-Power Amplifier Based on the Parallel Amplification Architecture for Electromagnetic Ultrasonic Guided Wave," *Sensors*, vol. 19, no. 13, p. 2924, Jul. 2019, doi: <https://doi.org/10.3390/s19132924>.
23. Y. Guo, C. Aquino, D. Zhang, and B. Murmann, "A Four-Channel, 36 V, 780 kHz Piezo Driver Chip for Structural Health Monitoring," *IEEE Journal of Solid-State Circuits*, vol. 49, no. 7, pp. 1506-1513, Apr. 2014, doi: <https://doi.org/10.1109/jssc.2014.2315615>.
24. P. R. Smith, D. M. J. Cowell, and S. Freear, "Width-modulated squarewave pulses for ultrasound applications," *IEEE Trans. Ultrason., Ferroelectr., Freq. Control*, vol. 60, no. 11, pp. 2244–2256, 2013. DOI: 10.1109/TUFFC.2013.6644730
25. M. Terenzi, D. Ghisu, F. Quaglia, E. Boni, M. Diaz Mendez, M. Valle, and D. D. Caviglia, "Flexible hardware architecture for the generation of ultrasound pulses in medical imaging," in 2016 *IEEE International Ultrasonics Symposium (IUS)*, 2016, pp. 1–4. DOI: 10.1109/ULTSYM.2016.7728595
26. P. Giannelli, A. Bulletti, M. Granato, G. Frattini, G. Calabrese and L. Capineri, "A Five-Level, 1-MHz, Class-D Ultrasonic Driver for Guided-Wave Transducer Arrays," in *IEEE Transactions on Ultrasonics, Ferroelectrics, and Frequency Control*, vol. 66, no. 10, pp. 1616-1624, Oct. 2019, doi: 10.1109/TUFFC.2019.2924943.

27. A. Bulletti, P. Giannelli, M. Calzolari and L. Capineri, "Multielement Interdigital Transducers for Structural Health Monitoring," 2018 IEEE International Ultrasonics Symposium (IUS), Kobe, Japan, 2018, pp. 1-3, [https://doi: 10.1109/ULTSYM.2018.8579613](https://doi.org/10.1109/ULTSYM.2018.8579613).

**Disclaimer/Publisher's Note:** The statements, opinions and data contained in all publications are solely those of the individual author(s) and contributor(s) and not of MDPI and/or the editor(s). MDPI and/or the editor(s) disclaim responsibility for any injury to people or property resulting from any ideas, methods, instructions or products referred to in the content.